Optical emission spectroscopic study of a steam arc cutting torch

V. Sember, A. Mašláni, P. Křenek, M. Hrabovský

[1]*Institute of Plasma Physics ASCR, Prague, Czech Republic*

Abstract: Optical emission spectroscopy has been used to investigate a plasma jet produced by a steam arc cutting torch operated in air at atmospheric pressure. A procedure has been developed for simultaneous determination of temperature and pressure in the plasma jet as well as a parameter characterizing the departure from LTE. It is based on comparison of a few experimental and simulated spectral quantities.

Keywords: plasma arc cutting, supersonic plasma jet, optical emission spectroscopy

1. Introduction

Plasma arc cutting (PAC) is a process that uses a highly constricted transferred dc arc established between the torch cathode and the work-piece acting as an anode through an extremely small nozzle bore. It was developed in the 1950s for cutting of metals that could not be cut by conventional oxy-fuel machines, such as stainless steels, aluminum and copper. Lots of commercial systems appeared during last fifteen years, which can successfully compete with laser and oxy-fuel ones.

During the last decade, a range of both theoretical and experimental studies has been published on this subject, nevertheless, experimental data on the PAC arc plasma are still rather scarce, e.g. [1-6]. There are two main reasons for this. First, in a real cutting configuration the distance between the nozzle exit and the work-piece is only a few millimeters, which together with the presence of metal vapors makes diagnostics of the arc column very difficult. This is usually circumvented by replacing the cutting work-piece with a rotating water-cooled metal disc located sufficiently far from the nozzle exit. Second, the cutting plasma jet is characterized by very small dimensions and supersonic flow conditions, resulting in steep temperature and density gradients, and departures from local thermodynamic equilibrium (LTE).

Under these conditions, applicability of most of methods developed for diagnostics of thermal plasma flows is therefore strongly limited. Up to now, only OES has been used for that purpose. Spectroscopic methods are, however, usually based on the assumption of LTE or partial LTE (pLTE) and care must be exercised when interpreting their results for this kind of plasma.

As the shock wave structure has an oblique pattern characteristic of underexpanded jets, the pressure has also non negligible radial gradients. Therefore, to determine plasma parameters in the supersonic part of the PAC jet, only those spectroscopic methods that do not depend on the pressure and LTE can be directly used. For example, Stark broadening and Boltzmann plot can be used for obtaining the electron number density or excitation temperature respectively. For some PAC configurations and operating conditions, other methods have been proposed that combine various spectroscopic measurements and theoretical calculations and the plasma parameters are obtained by means of an iterative procedure, e.g. [3].

In this paper we present a spectroscopic study of the plasma jet generated with the steam arc cutting torch. The evaluation method is based on comparison of a few experimental and simulated spectral quantities. The procedure enables the simultaneous determination of temperature and pressure in the plasma jet as well as a parameter characterizing the departure from LTE.

2. Experimental details

The steam dc arc cutting torch uses the mixture of water (about 80% by vol.) and ethyl alcohol as a working medium. The liquid is supplied into the torch where it passes an electric heating element, evaporates and the resulting steam flows along the cathode to the nozzle. Instead of the cutting work-piece, a water-cooled rotating copper disc was used as an anode. The anode disc is placed just behind the nozzle exit with its main axis and the circumferential surface oriented parallel to the plasma jet flow. The arc is transferred to the disc circumferential surface and the attachment occurs a few millimeters downstream of the nozzle. The torch was operated in air at atmospheric pressure and an arc current of 60 A.

Spectroscopic measurements are performed using a Jobin-Yvon imaging spectrograph Triax 550 equipped with a MTE CCD 1024x256 detector. The plasma jet is imaged by means of a lens on a line-to-line fiber optic cable consisting of 41 fibers, which is coupled to the entrance slit of the spectrograph with an imaging fiber adapter. A long-pass colored glass filter housed in a filter wheel attached to the spectrograph entrance is used to reduce the second order diffraction from the grating. The entire optical system is calibrated using a tungsten strip lamp.

Spatially resolved and time averaged spectra of the jet are taken along the line of sight perpendicular to the plane passing through the jet and the disc anode axes. If the plasma is optically thin and cylindrically symmetric, the measured spectral intensities can be converted to the local emission coefficients using an Abel inversion technique. To take into account a partial departure from the cylindrical symmetry caused the anode disc located downstream of the nozzle, a procedure developed by Yasutomo *et al* is used [7]. It assumes that the plasma keeps a cylindrical shape and an asymmetry exists only perpendicular to the direction of observation.

3. Spectroscopic Method

The experimental data were obtained from the spectrum centered at 480 nm, an example of which is shown in Fig. 1. It is dominated by very broad hydrogen Balmer H_β line and several O II lines. The following quantities were derived from the spectrum: full width at half maximum of H_β line (FWHM), maximum value of emission coefficient of H_β line $\varepsilon_{H\beta max}$, total emission coefficient of a group of O II lines 463.9-466.2 nm ε_{OII}, and ratio of H_β maximum and O II (463.9-466.2 nm) emission coefficients $\varepsilon_{H\beta max}/\varepsilon_{OII}$. The maximum of H_β line is defined as an average value of the blue and red maxima of the line after subtracting underlying continuum emission.

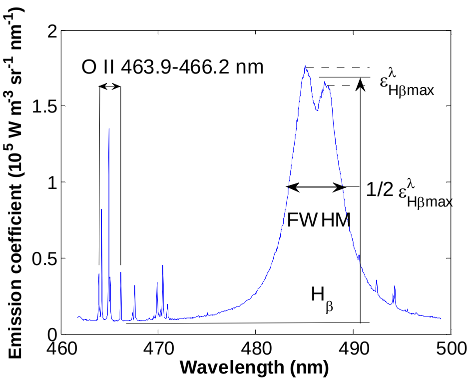

Fig. 1 Emission spectrum with H_β and O II lines.

The only parameter that can be derived directly from the spectroscopic data with no assumption about LTE is electron number density n_e, which can be obtained from FWHM of the H_β line. In our experimental conditions, the Stark broadening is by far the most effective mechanism contributing to the width of H_β line. The other mechanisms such as resonance, van der Waals, natural and instrumental broadening are quite negligible for $n_e > 10^{22}$ m^{-3}. Only a Doppler broadening has been taken into account. We have adopted an approximate formula for separation of the Doppler and Stark contributions to the resulting FWHM as given in [8]. The approximation assumes that the spectral line profile can be represented by a Voigt function resulting from a convolution of the Lorentz (Stark) and Gauss (Doppler) profiles. The Doppler width is calculated using the formula derived for H_β line in [9].

We have used the Stark widths listed by Gigosos and Cardeñoso [10], which were obtained by computer simulation technique with ion dynamics effects taken into account. For a range of plasma parameters prevailing in the jet core, the choice of temperature as an input parameter has negligible effect. The temperature was therefore set to a typical value obtained from a preliminary assessment.

The theoretical values of the measured emission coefficients were obtained using LTE composition calculated by the procedure described in [11]. The atomic data of transitions used for evaluation of $\varepsilon_{H\beta}$ and ε_{OII} were taken from [12]; and the corresponding partition functions were obtained from Drawin and Felenbok [13]. The value of $\varepsilon_{H\beta max}$ was determined from the total emission coefficient and the simulated line profile of H_β using the formula and tables of HWHM published by Vidal *et al* [14].

The procedure is based on fitting the radial profiles of

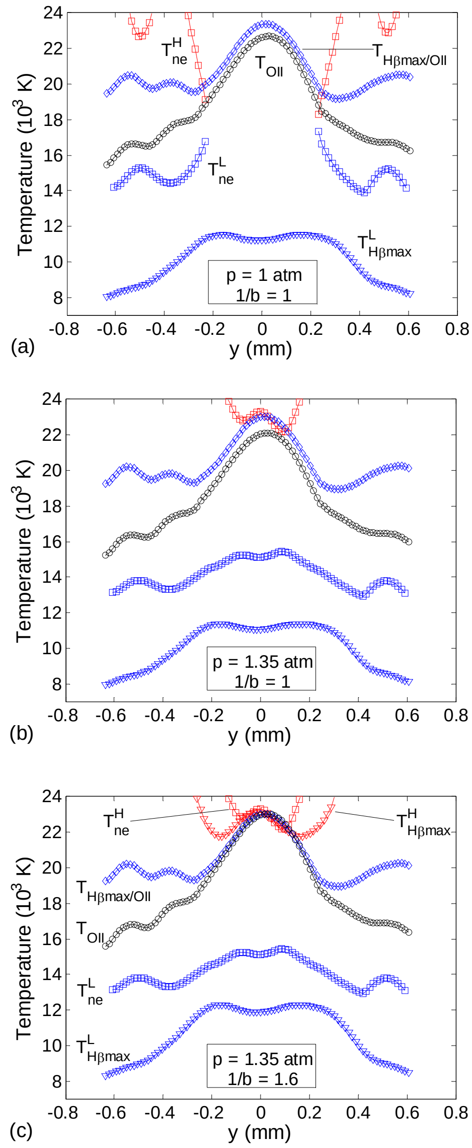

Fig. 2 Radial temperature profiles at the nozzle exit obtained from electron number density and absolute and relative emission coefficients of H_β and O II for the pressure (a) 1 atm, (b) 1.35 atm, and (c) 1.35 atm and absolute emission coefficients multiplied by a factor of 1.6.

temperatures obtained for each experimental quantity using the simulated data. First, theoretical values of the spectral quantities are calculated for a discrete set of temperatures and a given pressure using number densities of O II and H I from LTE composition. The temperature corresponding to each experimental quantity is then found by cubic spline interpolation on the theoretical data. This calculation is repeated for various pressures until the best fit between resulting radial temperature profiles is reached. To simplify the procedure without loosing the precision, we do not calculate the plasma composition for each pressure separately. Instead we use mole fractions of the species in question from the composition determined at atmospheric pressure, and the number densities for a particular pressure are derived using the perfect gas law. Except for the emission coefficient of O II lines, all other quantities peak at a certain temperature so that two solutions for the temperature can be obtained by the interpolation procedure, denoted as T^{L} and T^{H} for the lower and higher valued solution respectively.

The procedure is documented in Figs. 2(a)-(c). An agreement between the radial profiles of T_{ne} and $T_{H\beta max/OII}$ is chosen as a main criterion. The reason is that $\varepsilon_{H\beta max/OII}$ is almost independent of the pressure but is very sensitive to the temperature, and n_e is less sensitive to deviations from LTE than the absolute emission coefficients. The other criterion is that the fitting of temperature profiles is considered only within the centerline region ($-0.2 < y < 0.2$ mm) because of high uncertainty and ambiguity of the results out of this region. When the best fit between T_{ne} and $T_{H\beta max/OII}$ is reached, the temperatures obtained from the emission coefficients of $H_{\beta max}$ and O II lines remain either over- or underestimated with respect to the fitted temperature, as shown in Fig. 2(b). This is supposed to be attributed to the departure of excited state populations from LTE. An effective population factor b is found by multiplying the emission coefficients by a factor $1/b$ to get the best agreement between all the temperature profiles, as shown in Fig. 2(c).

4. Results and discussion

Two series of measurements were made along the jet centerline. The first one was more detailed, with a shorter step, and covered the first expansion region from the nozzle exit to the shock front. Figs. 3(a)-(c) show radial profiles of the temperatures determined from the measured spectral quantities at four distances from the nozzle exit: (a) at the nozzle exit; (b) in the middle of the first expansion; and (c) at the second shock front. The meaning of the curves is the same as explained in the previous section and below figure 2. But here all the values with controversial physical meaning are omitted so that the resulting temperature profile can be readily fitted to the curves.

Fig. 4(a) shows axial profiles of the pressure and temperature. It clearly indicates position of the first expansion

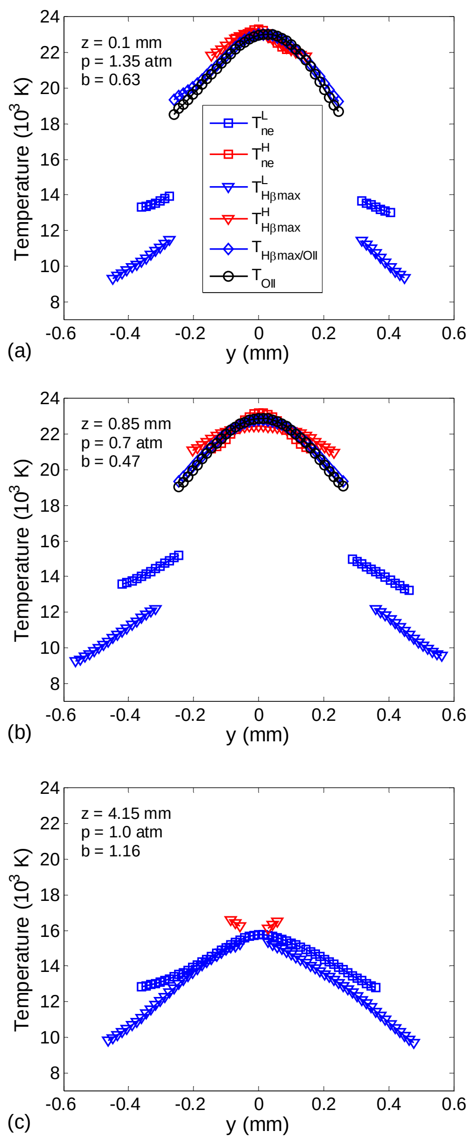

Fig. 3 Radial temperature profiles at three distances z from the nozzle exit.

region where the pressure drops from about 1.4 atm at the nozzle exit to about 0.7 atm at the distance of about 0.7 mm downstream of the nozzle. The expansion is followed by a shock front, after which another milder expansion and shock can be distinguished. This variation of the pressure with the exit pressure being higher than the surrounding pressure is typical for a supersonic underexpanded flow. The axial position of the first shock front can be checked by an empirical formula $z_s = 0.67\, d\, (p_e/p_b)$ given by Ashkenas *et al* [15], where p_e is the stagnation pressure at the torch exit, p_b the background pressure and d is the nozzle diameter. By putting $p_e = 1.4$ atm, $p_b = 1$ atm and $d = 1$ mm we obtain $z_s = 0.79$ mm which is in good agreement with the experimental value shown in Fig. 4(a). Contrary to the pressure, the temperature is almost constant in the first expansion region and starts to

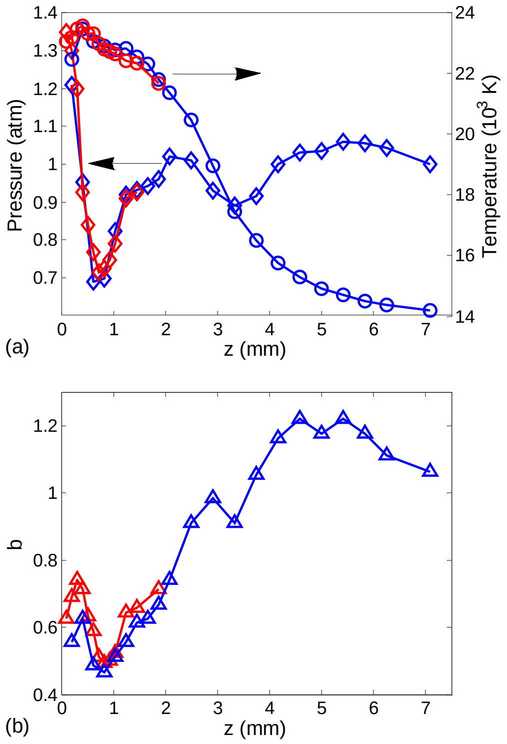

Fig. 4 Axial profiles of (a) the pressure and temperature and (b) the effective population factor.

decrease after the first shock front.

Axial profile of the effective population factor is shown in Fig. 4(b). There are two different regions in the plasma jet: the first one between the nozzle and the first shock in which the population factor is less than unity, and the second one in which it is higher than unity. In our case, the arc attachment occurs approximately at the distance of about 2 mm of the nozzle exit. The plasma between the nozzle and arc attachment is therefore still ionizing, which is characterized by underpopulation of the excited states with respect to the ionization equilibrium. The remaining part of the jet may be regarded as freely expanding and recombining plasma.

In fact, the population factor derived by our procedure is only a rough approximation to what is usually defined as the population factor; however, it seems to have a similar meaning. If this factor is not taken into account, the temperature derived from the absolute emission coefficient of oxygen ionic lines can be underestimated in the expansion region by as much as 1500 K.

In supersonic plasma jets there may be a significant departure from the thermal equilibrium. For example, the expansion of heavy particles is close to adiabatic while electrons are heated by Ohmic dissipation due to the charge separation in shock front and three-particle recombination. This may result in the strong drop of the heavy particle temperature in the expansion region with respect to the temperature of free electrons remain. From the present results and from the assumption that the populations of excited species can be in partial equilibrium with free electrons, we suppose the temperature we have obtained may be close to the temperature of free electrons.

5. Conclusion

The iterative procedure has been applied for simultaneous determination of the temperature, pressure and effective population parameter characterizing the departure from LTE. The procedure is based on the comparison of a few experimental and simulated spectral quantities using the LTE composition. In the centerline region of the plasma jet, our approach gives realistic values of the pressure comparable with other both experimental results and theoretical predictions. The axial profile of the temperature does not reveal any noticeable drop in the expansion region, which contradicts some experimental works, e.g. [4, 5], but it agrees with the turbulent model in [3].

References

[1] C. Pardo, J. González-Aguilar, A. Rodríguez-Yunta and M.A.G. Calderón, J. Phys. D: Appl. Phys. **32**, 2181-9 (1999).

[2] P. Freton, J.J. Gonzalez, A. Gleizes, F. Camy Peyret, G. Caillibotte and M. Delzenne, J. Phys. D: Appl. Phys. **35**, 115-31 (2002).

[3] P. Freton, J.J. Gonzalez, F. Camy Peyret and A. Gleizes, J. Phys. D: Appl. Phys. **36**, 1269-83 (2003).

[4] L. Girard, Ph. Teulet, M. Razafinimanana, A. Gleizes, F. Camy-Peyret, E. Baillot and F. Richard, J. Phys. D: Appl. Phys. **39**, 1543-56 (2006).

[5] J. Peters, J. Heberlein and J. Lindsay, J. Phys. D: Appl. Phys. **40**, 3960-71 (2007).

[6] J. Peters, B. Bartlett, J. Lindsay and J. Heberlein, Plasma Chem. Plasma Process. **28**, 331-52 (2008).

[7] Y. Yasutomo, K. Miyata, S.I. Himeno, T. Enoto and Y. Ozawa, IEEE Trans. Plasma Sci. **9**, 18-21 (1981).

[8] E.E. Whiting, J. Quant. Spectrosc. Radiat. Transfer **8**, 1379-84 (1968).

[9] C.O. Laux, T.G. Spence, C.H. Kruger and R. Zare, Plasma Sources Sci. Technol. **12**, 125-38 (2003).

[10] M.A. Gigosos and V. Cardeñoso, J. Phys. B: At. Mol. Opt. Phys. **29**, 4795-838 (1996).

[11] P. Křenek, Plasma Chemistry and Plasma Processing **28**, 107-122 (2008).

[12] http://physics.nist.gov/PhysRefData/ASD/ NIST Atomic Spectra Database.

[13] H.W. Drawin and P. Felenbok, Data for Plasmas in Local Thermodynamic Equilibrium, Paris: Gauthier--Villars (1965).

[14] C.R. Vidal, J. Cooper and E.W. Smith, Astrophys. J. Suppl. Ser. No. 214 **25**, 37-136 (1973).

[15] H. Ashkenas and F. Sherman, Proc. Rarefied Gasdynamics 4, ed J.H. de Leeuw, New York: Academic (1966).